Electroclinic effect in chiral SmA* liquid crystals induced by atropisomeric biphenyl dopants: amplification of the electroclinic coefficient using achiral additives†

C. Scott Hartley,[a] Nadia Kapernaum,[b] Jeffrey C. Roberts,[a] Frank Giesselmann[b] and Robert P. Lemieux*[a]

Received 27th October 2005, Accepted 29th March 2006
First published as an Advance Article on the web 24th April 2006
DOI: 10.1039/b515313a

The atropisomeric compound (*R*)-2,2′,6,6′-tetramethyl-3,3′-dinitro-4,4′-bis[(4-nonyloxybenzoyl)oxy]biphenyl ((*R*)-**1**) was doped in the achiral liquid crystal hosts 2-(4-butoxyphenyl)-5-octyloxypyrimidine (**2-PhP**) and 4-(4′-heptyl[1,1′-biphen]-4-yl)-1-hexylcyclohexanecarbonitrile (**NCB76**), and electroclinic coefficients e_c were measured as a function of the dopant mole fraction x_1 in the chiral SmA* phase at $T - T_C$ = +5 K. The extrapolated e_c values of 3.07 and 2.28 deg μm V^{-1} are comparable to some of the highest e_c values reported for neat SmA* materials. The electroclinic coefficient of a 4 mol% mixture of (*R*)-**1** in **2-PhP** is amplified by achiral 2-phenylpyrimidine additives (5 mol%) that are longer than **2-PhP**; in the best case, e_c is amplified by a factor of 3.2 with 5-(tetradecyloxy)-2-(4-(tetradecyloxy)phenyl)pyrimidine (**3g**), which is almost twice as long as **2-PhP**. However, no amplification is observed in a 4 mol% mixture of (*R*)-**1** in **NCB76** using the same series of additives. A correlation between e_c values and the temperature range of the SmA* phase suggests that the amplification of e_c with increasing length of the additive **3** in the (*R*)-**1**/**2-PhP** mixture is due primarily to a decrease in the tilt susceptibility coefficient α as the second-order SmA*–SmC* phase transition moves away from the tricritical point. Measurements of smectic layer spacing as a function of $T - T_C$ by small-angle X-ray scattering are consistent with this explanation. The results show that the variation in reduced layer spacing d_A/d_C with $T - T_C$ for the pure host **2-PhP** fits to a square-root law, which indicates that the second-order SmA–C transition is nearly tricritical. On the other hand, the corresponding variation in d_A/d_C with $T - T_C$ for a 5 mol% mixture of **3g** in **2-PhP** fits to a linear relation, which indicates that the second-order SmA–C transition approaches typical mean-field behavior.

Introduction

The electroclinic effect is a unique and technologically useful electro-optical property of the chiral smectic A (SmA*) liquid crystal phase.[1] The SmA* phase is characterized by a diffuse layer structure in which the molecular long axes of chiral mesogens are oriented perpendicular to the layer plane, on the time-average, and it cannot be distinguished from the achiral SmA phase in the absence of external perturbations. However, Garoff and Meyer showed that an electric field E applied parallel to the layers of a chiral SmA* phase induces a molecular tilt θ relative to the layer normal in a direction orthogonal to the field.[2] This electroclinic effect is described by a phenomenological model derived from Landau theory which predicts a linear dependence of the induced tilt angle θ on the applied field E at low field strengths.[3] This relationship is expressed by eqn (1) and (2),

$$\theta = e_c E \quad (1)$$

$$e_c = \frac{c}{\alpha(T - T_C)} \quad (2)$$

where e_c is the electroclinic coefficient, c is the electroclinic coupling constant, and $\alpha(T - T_C)$ is the first coefficient of the Landau free-energy expansion. The term α is a nonchiral parameter known as the tilt susceptibility coefficient, or tilt elastic modulus, which describes the restoring torque taking the director back to the layer normal. The term c is a chiral parameter describing the coupling between the spontaneous polarization and the tilt θ in the SmC* phase.[1] The relationship between θ and E normally deviates from linearity at high field strengths and/or when the temperature approaches the Curie point T_C corresponding to the second-order transition from the orthogonal SmA* to the tilted SmC* phase.

The linear relationship between the induced electroclinic tilt and E at low field strengths makes it possible to generate a gray scale display between crossed polarizers, and its response time may be orders of magnitude faster than a

[a]*Chemistry Department, Queen's University, Kingston, Ontario, Canada K7L 3N6*
[b]*Institute of Physical Chemistry, Universität Stuttgart, Pfaffenwaldring 55, D-70569, Stuttgart, Germany*

† Electronic supplementary information (ESI) available: synthetic procedures and spectral characterization data (^{1}H and ^{13}C NMR, low- and high-resolution MS) for compounds **3a–h**. See DOI: 10.1039/b515313a

surface-stabilized ferroelectric liquid crystal (SSFLC) display.[4] Such properties make electroclinic SmA* materials suitable for a wide range of electro-optical device applications, including micro-color filters, tunable color filters and spatial light modulators.[5] To develop electroclinic materials for device applications, several groups have focused their efforts on the design of chiral SmA* liquid crystals with high electroclinic coefficients,[6–10] including de Vries SmA* liquid crystals, which are characterized by a tilted molecular orientation with random azimuthal distribution.[11–19] However, the design of SmA* liquid crystals suitable for device applications is a multi-variable problem that also requires the optimization of achiral parameters unrelated to the electroclinic properties. A solution to this problem, which is widely used in the formulation of ferroelectric SmC* liquid crystals for SSFLC display applications,[20] is to combine a chiral dopant that induces the desired electroclinic response at low concentration with an achiral SmA liquid crystal host mixture.[21–23]

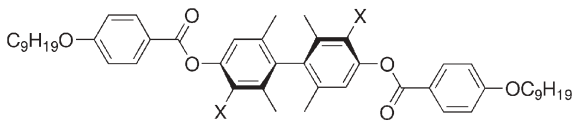

1, X = NO_2
2, X = Me

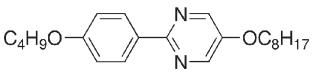

2-PhP: Cr 58 SmC 85 SmA 95 N 98 I

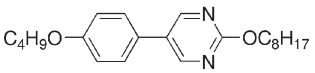

5-PhP: Cr 84 SmA 117 I

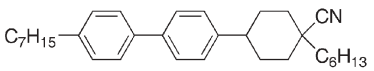

NCB76: Cr 66 (SmG 55) SmC 73 SmA 117 N 125 I

In general, SmA* liquid crystals with large e_c values exhibit large spontaneous polarizations in the SmC* phase. We have shown that chiral dopants with atropisomeric biphenyl cores such as **1** induce ferroelectric SmC* phases and exhibit remarkably high polarization powers (δ_p)—up to 1738 nC cm^{-2}—in achiral SmC liquid crystal hosts with a complementary phenylpyrimidine core structure in which the atropisomeric core propagates its chirality through core–core interactions with surrounding host molecules.[24,25] The resulting chiral perturbations are thought to amplify the induced polarization as a feedback effect (Chirality Transfer Feedback, CTF) by causing a shift in the conformational distribution of the chiral dopant favoring one orientation of its transverse dipole moment along the polar axis of the SmC* phase. Evidence supporting the CTF amplification was provided by probe experiments in which the polarization powers of (*R*) and (*S*) enantiomers of a probe dopant exerting much weaker chiral perturbations (the probe **2**) were measured in the presence of (*S*)-**1** at a constant mole fraction of $x_1 = 0.04$ (4 mol%) in **2-PhP**.[26] In the presence of (*S*)-**1**, the polarization powers of (*R*)-**2** and (*S*)-**2** increase by factors of 5.5 and 2.8, respectively, and the sign of polarization induced by (*S*)-**2** is inverted from negative to positive. These results reflect the diastereomeric relationship between the two dopant/probe combinations, and are consistent with long range *chiral* perturbations amplifying the polarization power of **2**.

As part of a broader study on the influence of the SmC host composition on polarization amplification in the SmC* phase, we recently showed that dopant **1** induces an electroclinic effect in mixtures of **2-PhP** and **5-PhP** that scales with the mole fraction of the latter; at a dopant mole fraction of $x_1 = 0.04$, the electroclinic coefficient e_c at 5 K above the Curie point ($T - T_C = +5$ K) ranges from 0.06 deg μm V^{-1} ($x_{5\text{-PhP}} = 0.0$) to 0.34 deg μm V^{-1} ($x_{5\text{-PhP}} = 0.24$).[27] The increase in e_c was originally attributed to a more effective propagation of chiral perturbations *via* interactions with the non-planar 5-phenylpyrimidine core, and implied that CTF amplification is also operative in the chiral SmA* phase. In this paper, we report a more complete assessment of the propensity of **1** to induce an electroclinic effect in achiral SmC hosts that refutes our original explanation, and ultimately addresses a question of fundamental importance: does the SmA* phase under an electric field have the same structure as the SmC* phase?[28–30] In addition, we report a large amplification of e_c in 4 mol% mixtures of (*R*)-**1** in the unsymmetrically substituted host **2-PhP** upon addition of symmetrically substituted 2-phenylpyrimidine mesogens that cause a broadening of the temperature range of the SmA* phase.

Results and discussion

Electroclinic coefficient measurements

Mixtures of (*R*)-**1** in the achiral hosts **2-PhP** and **NCB76** were prepared, with dopant mole fractions in the ranges of $0.04 \leqslant x_1 \leqslant 0.2$ and $0.02 \leqslant x_1 \leqslant 0.08$, respectively. The mixtures were aligned in commercial ITO glass cells with parallel-rubbed polyimide surfaces and a spacing of 4 μm. Electroclinic tilt angles θ were measured at $T - T_C = +5$ K by polarized optical microscopy (POM) as half the rotation between the two extinction positions observed upon applying a 0.1 Hz square wave ac field E ranging from 0 to 15 V μm^{-1}. In most cases, plots of θ *vs.* E gave good linear least-squares fits from which e_c values were derived according to eqn (1). Samples at the high end of the x_1 ranges gave plots of θ *vs.* E that deviate from linearity at high fields; in those cases, the linear portions of the plots were used to determine e_c values. Plots of e_c *vs.* x_1 in **2-PhP** and **NCB76** gave good least-squares fits ($R^2 = 0.991$ and 0.999, respectively), as shown in Fig. 1. Due to the paucity of studies reporting electroclinic coefficients for induced SmA* phases, it is difficult to assess the effectiveness of **1** as an electroclinic chiral dopant. Nevertheless, extrapolations of e_c to $x_1 = 1.0$ according to the least-squares fits give values of 3.07 ± 0.17 deg μm V^{-1} in **2-PhP** and 2.28 ± 0.06 deg μm V^{-1} in **NCB76**, which are of the same order of magnitude as the highest electroclinic coefficients reported for neat SmA* liquid crystals (on the order of 6–7 deg μm V^{-1} at the same reduced temperature).[12,31]

The difference in extrapolated e_c values measured in the hosts **2-PhP** and **NCB76** is much smaller than the

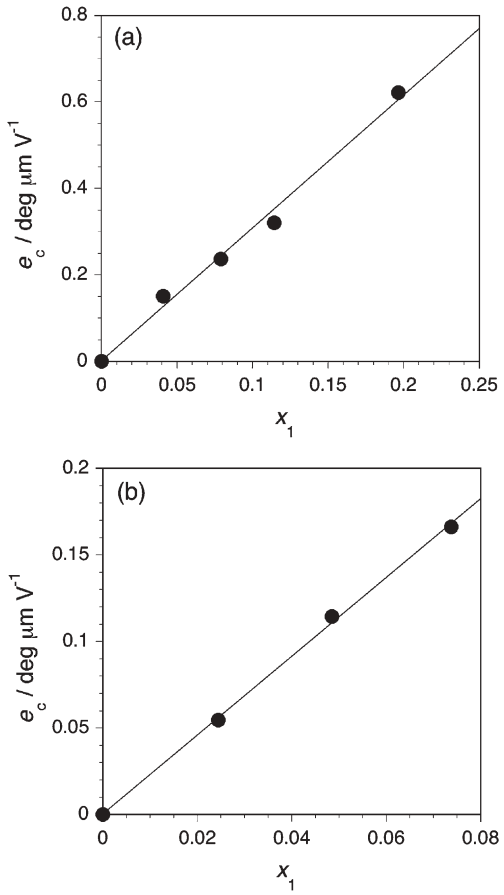

Fig. 1 Electroclinic coefficient e_c *vs.* mole fraction of (*R*)-**1** x_1 in (a) **2-PhP** and (b) **NCB76** measured at $T - T_C = +5$ K. The lines represent the least-squares fits to the data.

corresponding difference in δ_p values (−1555 *vs.* −514 nC cm^{-2}, respectively), which suggests that the CTF effect may not play as important a role in the SmA* phase as in the SmC* phase.[32] To determine the influence of chiral perturbations exerted by (*R*)-**1** on the induced electroclinic effect in **2-PhP**, we performed probe experiments using mixtures of (*R*)-**1** (x_1 = 0.04) and either the (*R*) or (*S*) enantiomer of the probe dopant **2** (x_2 = 0.03) in the host **2-PhP**. Four replicate mixtures were prepared for each dopant combination, and electroclinic coefficients were measured for each mixture at $T - T_C = +1.5$, +2.5 and +5 K, and plotted as a function of $T - T_C$. As shown in Fig. 2, there is no significant difference between e_c values for the (*R*,*R*) and (*R*,*S*) dopant/probe combinations, which indicates that the contribution of the chiral dopant **2** to the induced electroclinic effect is too small to be measured at x_2 = 0.03, and suggests that (*R*)-**1** does not exert long range chiral perturbations in the SmA* phase that would amplify the contribution of **2** to the induced electroclinic effect. This result is consistent with the less pronounced host dependence exhibited by e_c relative to δ_p, and implies that the degree of core–core correlation in the SmA* phase under an electric field is significantly less than in the tilted SmC* phase. This would be consistent with previous observations that molecules tilt as rigid rods in the SmA* phase under an electric field,[28,29] and are therefore more prone

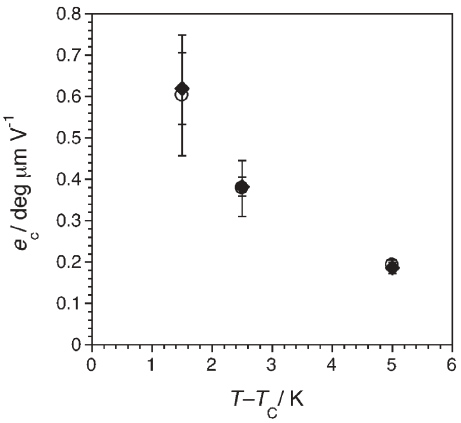

Fig. 2 Electroclinic coefficient e_c *vs.* reduced temperature $T - T_C$ for mixtures of (*R*)-**1** (x_1 = 0.04) and (*R*)-**2** (x_2 = 0.03) (filled diamonds), and (*R*)-**1** (x_1 = 0.04) and (*S*)-**2** (x_2 = 0.03) (open circles) in **2-PhP**. The error bars represent the 95% confidence limit about each point.

to out-of-layer fluctuations than in the SmC* phase, in which the tails are less tilted than the core.[33] However, these results do not rule out completely the contribution of CTF to the electroclinic effect, but suggest that any chiral perturbations exerted by (*R*)-**1** in the SmA* phase are on a much shorter length scale due to less effective core–core interactions.

Although there is no evidence that dopant **2** has a significant 'chiral' influence on the electroclinic effect of the 4 mol% mixture of (*R*)-**1** in **2-PhP**, the electroclinic coefficient of the mixture does increase significantly in the presence of either enantiomer of **2** at x_2 = 0.03 (0.19 *vs.* 0.12 deg μm V^{-1} at $T - T_C = +5$ K). Since the dopant molecules **1** and **2** are significantly longer than the host molecules (*ca.* 47 Å for **1** and **2** *vs.* 26 Å for **2-PhP** and 28 Å for **NCB76**), we sought to determine whether this discrepancy in molecular length plays a role in the induction of the relatively large electroclinic effects reported herein. To investigate the effect of molecular length discrepancy systematically, we synthesized a series of 2-phenylpyrimidine mesogens **3a–h**, which are approximately equal to or greater in length than **2-PhP** and **NCB76**, and measured the effect of these additives on the electroclinic coefficient in 4 mol% mixtures of (*R*)-**1** in **2-PhP** and **NCB76**.

Compounds **3a–h** were prepared by dialkylation of 2-(4-hydroxyphenyl)-5-pyrimidol. Their phase transition temperatures were measured by differential scanning calorimetry, and the mesophases identified by texture analysis using POM (Table 1). The compounds **3a–f** are known and, with the exception of **3a**, the phase sequences and transition temperatures are in good agreement with the literature values.[34] The phase sequences follow the expected empirical trend, *i.e.*, a stabilization of the SmC phase at the expense of the nematic and SmA phases with increasing chain length. Mixtures of (*R*)-**1** (x_1 = 0.04) and **3a–h** (x_3 = 0.05) in the hosts **2-PhP** and **NCB76** were prepared and analyzed by POM; all eight additives were used in the (*R*)-**1/2-PhP** series, but only **3b**, **3d**, **3f** and **3g** were used in the (*R*)-**1/NCB76** series. As shown in the phase diagrams in Fig. 3, the increase in chain length *n* of the additive **3** has relatively little effect on the I–N* and N*–SmA* phase transition temperatures in **2-PhP** and **NCB76**, but causes a significant decrease in the SmA*–SmC*

Table 1 Liquid crystal properties and molecular lengths of achiral additives **3a–h**

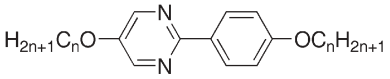

3a-h

Additive	n	Length/Å[a]	Phase sequence (°C)[b]
3a	6	25.6	Cr 69 SmC 74 SmA 77 N 100 I
3b	8	30.6	Cr 53 SmC 93 SmA 101 N 102 I
3c	9	33.1	Cr 64 SmC 97 SmA 101 I
3d	10	35.5	Cr 58 SmC 104 I
3e	11	38.1	Cr 74 SmC 103 I
3f	12	40.5	Cr 66 SmC 105 I
3g	14	45.5	Cr 77 SmC 104 I
3h	16	50.5	Cr 85 SmX[c] 86 SmC 102 I

[a] Derived from AM1-minimized molecular models. [b] Determined by differential scanning calorimetry and polarized microscopy. [c] Unidentified higher order smectic phase.

phase transition temperature in **2-PhP**, resulting in a broadening of the SmA* phase. By comparison, the increase in chain length of **3** has little effect on the SmA*–SmC* phase transition temperature in **NCB76**.

The electroclinic coefficients of these mixtures were measured at $T - T_C$ = +5 K and plotted as a function of the additive chain length n. As shown in Fig. 4, the electroclinic coefficient increases with the chain length of **3** in the (*R*)-**1/2-PhP** mixture and reaches a maximum of 0.38 deg μm V^{-1} at

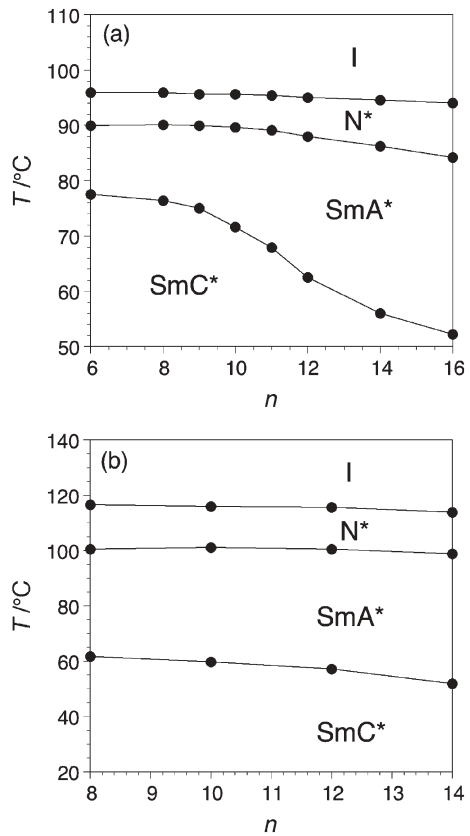

Fig. 3 Phase diagrams for mixtures of (*R*)-**1** (x_1 = 0.04) and **3** (x_3 = 0.05) in the hosts (a) **2-PhP** and (b) **NCB76** as a function of the chain length n of **3**.

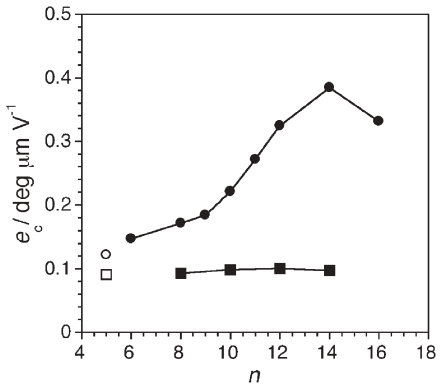

Fig. 4 Electroclinic coefficient e_c *vs.* additive chain length n for mixtures of (*R*)-**1** (x_1 = 0.04) and **3** (x_3 = 0.05) in the hosts **2-PhP** (filled circles) and **NCB76** (filled squares). The open symbols represent the electroclinic coefficients in the absence of additive.

n = 14, which is 3.2 times larger than the electroclinic effect achieved without additive. On the other hand, the additives have no effect on the electroclinic coefficient in the (*R*)-**1/NCB76** mixture, despite the fact that they are all longer than the host. Plots of e_c *vs.* $T - T_C$ for (*R*)-**1/2-PhP** mixtures with the additives **3a**, **3d** and **3g** give excellent fits to eqn (2) (R^2 > 0.98), with c/α values of 0.66, 1.03 and 1.88 deg K μm V^{-1}, respectively (Fig. 5). If we consider the results of the probe experiments, which suggest that chirality transfer does not contribute to the electroclinic effect in the SmA* phase, it is reasonable to assume that the chirality-dependent electroclinic coupling constant c is invariant in this series of mixtures, and that the electroclinic amplification effect results primarily from a decrease in the tilt susceptibility coefficient α.

Why do we observe an amplification in e_c with increasing chain length of **3** in the (*R*)-**1/2-PhP** mixture, but not in the (*R*)-**1/NCB76** mixture? Literature precedents paint a rather inconsistent picture of the relationship between the chain length of SmA* component(s) and the magnitude of e_c. Several studies have shown that the electroclinic coefficients of homologous series of SmA* mesogens increase with the length

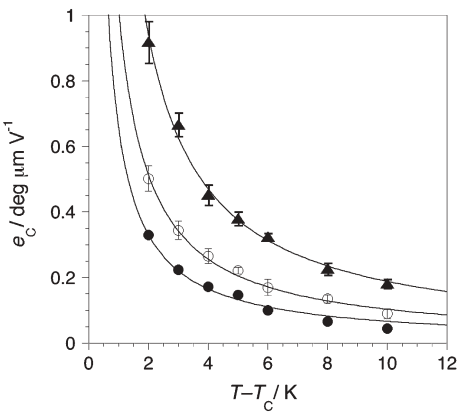

Fig. 5 Electroclinic coefficient e_c *vs.* reduced temperature $T - T_C$ for mixtures of (*R*)-**1** (x_1 = 0.04) and **3** (x_3 = 0.05; **a**, filled circles; **d**, open circles; **g**, triangles) in **2-PhP**. The lines show the least-squares fits to eqn (2) (**a**, c/α = 0.66 ± 0.02 deg K μm V^{-1}; **d**, c/α = 1.03 ± 0.01 deg K μm V^{-1}; **g**, c/α = 1.88 ± 0.03 deg K μm V^{-1}).

of chiral and achiral side-chains,[7,35,36] which was attributed to an increase in molecular flexibility that imparts a greater mobility to the aromatic cores.[35] On the other hand, Beresnev *et al.* reported a decrease in e_c upon lengthening the side-chains of a chiral dopant (10% w/w) in a three-component SmA* mixture.[37] Kang *et al.* also reported a decrease in e_c upon similar modification of a chiral dopant (5% w/w) in a SmA host.[23] In the present case, the amplification of e_c may be explained by considering the effect of the additive on the temperature range of the SmA* phase. In liquid crystals with I–N–SmA–SmC or I–SmA–SmC phase sequences, it is well known that the second order SmA–C phase transition approaches the tricritical point (crossover from second to first order), and ultimately becomes discontinuous (first order), as the temperature range of the SmA phase decreases.[38–41] In the chiral SmA* phase, the approach of a SmA*–C* phase transition towards the tricritical point (tricritical transition) causes an increase in α as the fluctuations in tilt θ near the SmA*–C* phase transition decrease in magnitude.[42] In the (*R*)-**1/2-PhP** mixtures, the increase in e_c with increasing chain length of the additive **3** correlates with a broadening of the SmA* temperature range except at very long chain length (**3h**), which suggests that the amplification effect is due primarily to a decrease in α as the second order SmA*–C* phase transition moves away from the tricritical point. In the (*R*)-**1/NCB76** mixtures, the lengthening of the additive **3** has relatively little effect on the SmA* temperature range, and on the corresponding electroclinic coefficient, which is consistent with this explanation. Indeed, the amplification of e_c first observed with mixtures of (*R*)-**1** in **2-PhP** and **5-PhP** can also be correlated to a broadening of the SmA* temperature range with increasing proportion of **5-PhP**,[43] which suggests that our original explanation of this effect based on enhanced chirality transfer in the SmA* phase is incorrect.[27]

SAXS measurements

To investigate the effects of additives **3a** and **3g** on the SmA–C phase transition of **2-PhP**, the smectic layer spacings d of pure **2-PhP**, **3a**, **3g** and 5 mol% mixtures of **3a** in **2-PhP** and **3g** in **2-PhP** were measured as a function of temperature by small-angle X-ray scattering (SAXS). As shown in Fig. 6, the layer spacing of pure **2-PhP** undergoes substantial shrinkage below the SmA–C phase transition temperature T_C (86 °C); at $T - T_C = -20$ K, the layer spacing d_C is reduced by 1.8 Å (*ca.* 7%) relative to the extrapolated layer spacing d_A of the SmA phase (dashed line). By contrast, the layer spacing d_C of the additive **3g**, which undergoes a first-order transition from isotropic liquid to the SmC phase at 102 °C, increases sharply due to the rapidly increasing orientational order expected for such materials on cooling from the isotropic liquid phase. When compared to the two pure components, the mesomorphic properties of the 5 mol% mixture of **3g** in **2-PhP** show some remarkable features: (i) a lowering of the SmA–C transition temperature by more than 20 K relative to that of pure **2-PhP** and a broadening of the SmA temperature range despite the fact that pure **3g** forms only a SmC phase that is stable at much higher temperatures; (ii) a reduction in layer shrinkage in the SmC phase from 7% (pure **2-PhP**) to 4% at

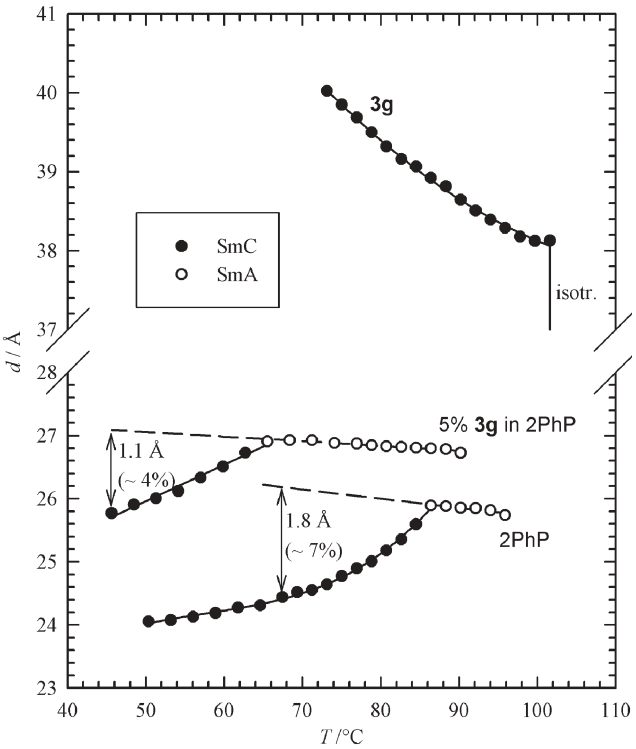

Fig. 6 Smectic layer spacing d *vs.* temperature T for pure **2-PhP**, **3g**, and a 5 mol% mixture of **3g** in **2-PhP**.

$T - T_C = -20$ K; and (iii) a near linear variation in d_C with temperature that stands in sharp contrast to the concave curvature shown in the $d_C(T)$ plot of pure **2-PhP**, the latter being typical of most materials with second-order SmA–C transitions.

The change in profile of the $d_C(T)$ plots is consistent with a change in the nature of the SmA–C transition. If we assume in a first approximation that the mesogenic molecules behave as rigid rods, the tilt angle θ formed by the molecular long axes and the layer normal in the SmC phase reduces the layer spacing d_C to:

$$d_C = d_A \cos\theta \tag{3}$$

based on simple geometry considerations. For small tilt angles θ, eqn (3) can be expanded as:

$$d_C = d_A\left(1 - \frac{\theta^2}{2} + \ldots\right) \tag{4}$$

or:

$$\frac{d_C}{d_A} \approx 1 - \frac{\theta^2}{2} \tag{5}$$

Since θ is the primary order parameter describing the SmA–C phase transition, the temperature variation of θ is described according to the general power law:

$$\theta \propto |T - T_c|^{\beta} \tag{6}$$

where T_c is the SmA–C transition temperature (critical temperature), and the order parameter exponent β is related

to the nature of the phase transition. According to the generalized mean-field theory of phase transitions (Landau theory), a β value of ½ is expected in the case of a pure second-order transition (mean-field transition), whereas a β value of ¼ is expected in the case of a second-order transition approaching the tricritical point (tricritical transition).[44,45] We therefore obtain:

$$\theta^2 \propto \begin{cases} |T-T_c| & \text{mean-field} \\ |T-T_c|^{1/2} & \text{tricritical} \end{cases} \quad (7)$$

By inserting these results into eqn (8), we find that:

$$\frac{d_C}{d_A} \approx \begin{cases} 1-a|T-T_c| & \text{mean-field} \\ 1-a|T-T_c|^{1/2} & \text{tricritical} \end{cases} \quad (8)$$

where a is a proportionality constant. According to this result, the reduced layer spacing d_C/d_A should vary linearly with temperature in the case of a pure mean-field transition (at small tilt angles); in the borderline case of a tricritical transition, a square-root law is expected. These considerations are applied to our experimental data in Fig. 7, where d_C/d_A is plotted against the reduced temperature $T - T_C$, and compared to the best fits to eqn (8). As shown in Fig. 7a, the $d_C/d_A(T - T_C)$ plot for the pure host **2-PhP** fits to the square-root law in eqn (8), which indicates that the second-order SmA–C transition in **2-PhP** is nearly tricritical. On the other hand, the $d_C/d_A(T - T_C)$ plot for the 5 mol% mixture of **3g** in **2-PhP** fits to the linear relation in eqn (8) (at least for small θ values), which indicates that the second-order SmA–C phase transition approaches the mean-field limit according to Landau theory. These results are consistent with the broadening of the SmA phase observed upon addition of **3g** to **2-PhP**, and the corresponding enhancement of the electroclinic coefficient.

To clarify whether this effect depends on the molecular length of the additive, we studied the effect of the shorter additive **3a**, which also undergoes a SmA–C transition, on the smectic layer spacing of **2-PhP**. As shown in Fig. 8, the layer spacing of pure **3a** undergoes substantial shrinkage below the SmA–C phase transition; at $T - T_C = -7$ K, the layer spacing d_C is reduced by 1.5 Å (*ca.* 6%) relative to the extrapolated layer spacing d_A of the SmA phase, which is even greater than that measured for **2-PhP** at the same reduced temperature (*ca.* 4%). At the SmA–C transition temperature T_C, the layer spacings of the two pure materials are approximately the same (*ca.* 25.8 Å). The extent of layer shrinkage of a 5 mol% mixture of **3a** in **2-PhP** at $T - T_C = = -7$ K is approximately the same as that of pure **2-PhP**, and the temperature dependence of d_C appears to be similar in character. However, the layer spacing of the mixture is *ca.* 0.5 Å smaller than for pure **2-PhP**, which violates the empirical trend described by the 'additivity rule' of Diele that gives the layer spacing of a smectic mixture as the weighted average of the layer spacings of the pure components.[46] In this case, the SAXS data suggest that the addition of **3a** substantially reduces the orientational order of the pure host and, consequently, its smectic layer spacing.[14]

As shown in Fig. 9, the $d_C/d_A(T - T_C)$ plot for the 5 mol% mixture of **3a** in **2-PhP** fits to the square-root law in eqn (8). This suggests that the nature of the SmA–C phase transition is similar to that of the pure host—near the tricritical point—which is consistent with the negligible e_c amplification observed with this mixture.

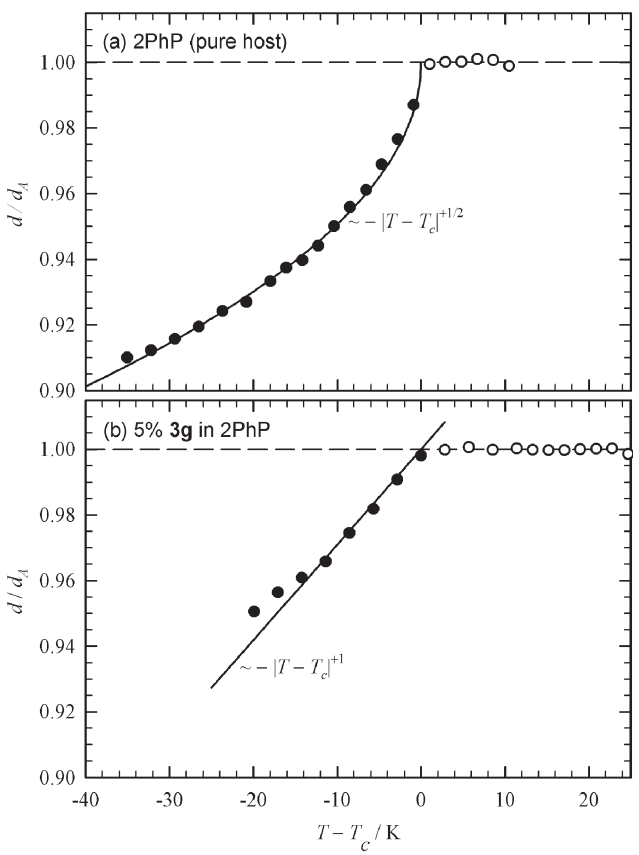

Fig. 7 Reduced layer spacing d_C/d_A *vs.* reduced temperature $T - T_C$ for (a) pure **2-PhP** and (b) a 5 mol% mixture of **3g** in **2-PhP**. The solid lines represent the fits to eqn (8) for tricritical and mean-field transitions, respectively.

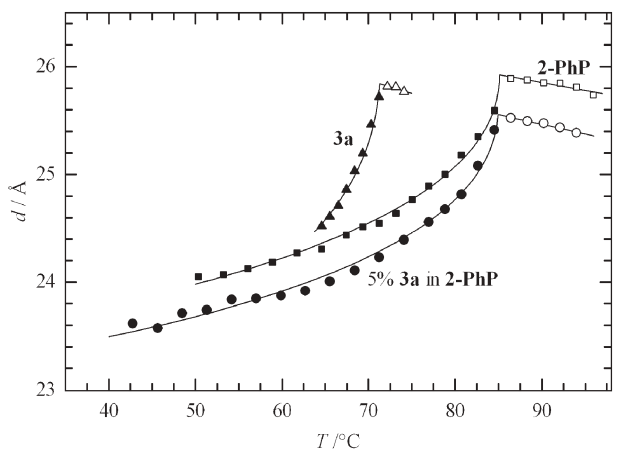

Fig. 8 Layer spacing d *vs.* temperature T in the SmA (open symbols) and SmC (filled symbols) phases for pure **2-PhP** (squares), **3a** (triangles) and a 5 mol% mixture of **3a** in **2-PhP** (circles).

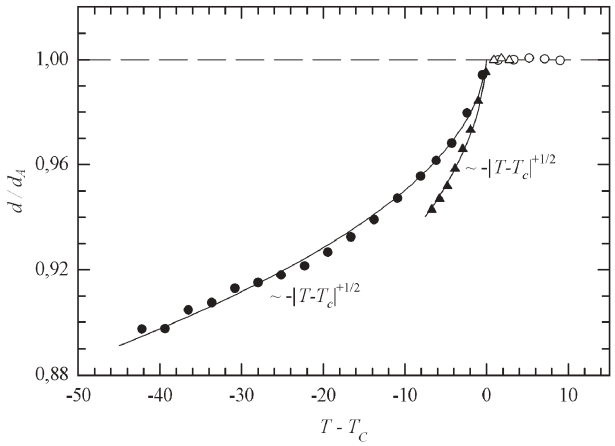

Fig. 9 Reduced layer spacing d_C/d_A *vs.* reduced temperature $T - T_C$ for the additive **3a** (triangles) and a 5 mol% mixture of **3a** in **2-PhP** (circles). The solid lines represent the fits to eqn (8) for tricritical transitions.

Spontaneous polarization measurements

The spontaneous polarization (P_S) of the chiral SmC* phase is considered to be a secondary order parameter of the SmA*–C* phase transition.[47] Due to the coupling between P_S and θ, the temperature dependence of P_S near T_C should also reflect the nature of the SmA*–C* phase transition. However, P_S measurements by integration of polarization reversal current peaks are complicated by induced polarization contributions near T_C due to the electroclinic effect (soft mode),[48] although the latter can often be minimized by using low triangular ac fields. The $P_S(T - T_C)$ plot for the 5 mol% mixture of **3a** in **2-PhP** (Fig. 10a) was obtained using the lowest possible triangular ac field (2 V μm^{-1}) without compromising the accuracy of the current peak integration. Despite the low ac field, the plot still shows some tailing beyond T_C that results from the soft mode contribution to the polarization reversal current. By comparison, the $P_S(T - T_C)$ plot for the 5 mol% mixture of **3g** in **2-PhP** (Fig. 10b) shows a much more pronounced tailing beyond T_C that precludes any attempt at fitting the plot to a power law similar to eqn (6). The pronounced distortion of this plot near the SmA*–C* transition is consistent with the higher electroclinic effect observed with this mixture, but it makes impossible any useful comparison to the $P_S(T)$ profile in Fig. 10a.

Summary

The atropisomeric dopant (*R*)-**1** induces an electroclinic effect in the liquid crystal hosts **2-PhP** and **NCB76** with extrapolated electroclinic coefficients e_c of 3.07 and 2.28 deg μm V^{-1} at $T - T_C = +5$ K, respectively, which are comparable to some of the highest e_c values reported for neat SmA* materials. In contrast to the polarization power δ_p of (*R*)-**1** in the SmC* phase, e_c is much less sensitive to the host structure. Furthermore, the results of probe experiments with (*R*)-**2** and (*S*)-**2** suggest that any chiral perturbation exerted by (*R*)-**1** in the SmA* phase under an electric field must be on a shorter length scale than in the SmC* phase, which is consistent with

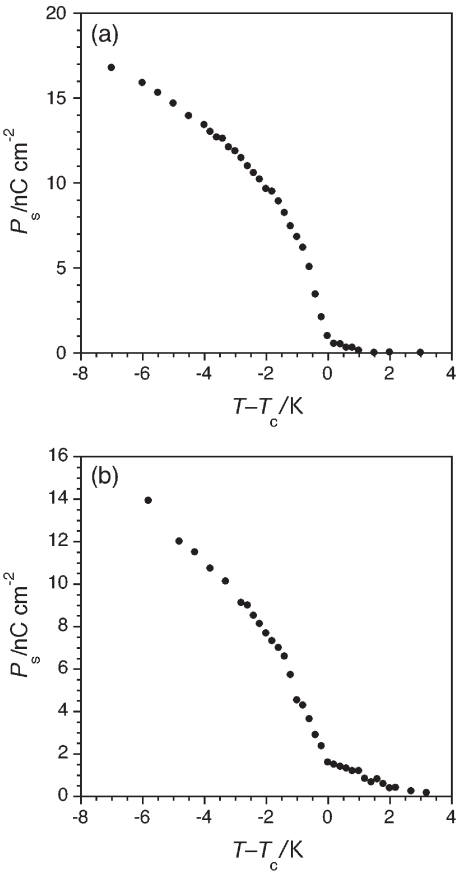

Fig. 10 Spontaneous polarization P_S *vs.* reduced temperature $T - T_C$ for mixtures of (a) (*R*)-**1** ($x_1 = 0.04$) and **3a** ($x_3 = 0.05$) in **2-PhP** and (b) (*R*)-**1** ($x_1 = 0.04$) and **3g** ($x_3 = 0.05$) in **2-PhP**. The spontaneous polarizations were measured using a triangular ac field of 2 V μm^{-1}.

previous observations that molecules tilt as rigid rods in the SmA* phase under an electric field.[28,29] The electroclinic coefficient of a 4 mol% mixture of (*R*)-**1** in **2-PhP** is amplified by achiral 2-phenylpyrimidine additives that are longer than **2-PhP**; in the best case, e_c is amplified by a factor of 3.2 with the bis-tetradecyloxy derivative **3g**, which is almost twice as long as **2-PhP**. However, no amplification is observed in 4 mol% mixtures of (*R*)-**1** in **NCB76** using the same series of additives.

A correlation between e_c values and the temperature range of the SmA* phase suggests that the amplification of e_c with increasing length of the additive **3** in the (*R*)-**1**/**2-PhP** mixture is due primarily to a decrease in the tilt susceptibility coefficient α as the second-order SmA*–SmC* phase transition moves away from the tricritical point. Measurements of smectic layer spacing as a function of $T - T_C$ by SAXS are consistent with this explanation. The results show that the variation in reduced layer spacing d_A/d_C with $T - T_C$ for the pure host **2-PhP** fits to a square-root law, which indicates that the second-order SmA–C transition is nearly tricritical. On the other hand, the corresponding variation in d_A/d_C with $T - T_C$ for a 5 mol% mixture of **3g** in **2-PhP** fits to a linear relation, which indicates that the second-order SmA–C transition approaches typical mean-field behavior. Further work aimed at establishing the generality of this effect in SmA* phases with

large electroclinic coefficients is in progress and will be reported in due course.

Experimental

Materials

Dopants (*R*)-**1**, (*R*)-**2** and (*S*)-**2** were synthesized according to published procedures and shown to have the expected physical and spectral properties.[32,49] The liquid crystal hosts 2-(4-butoxyphenyl)-5-octyloxypyrimidine (**2-PhP**) and 4-(4′-heptyl[1,1′-biphen]-4-yl)-1-hexylcyclohexanecarbonitrile (**NCB76**) were obtained from commercial sources. Synthetic procedures and spectral data for compounds **3a–h** are described in the Electronic Supplementary Information.†

Physical measurements

Differential scanning calorimetry analyses were performed at a scan rate of 5 K min^{-1} on a Perkin-Elmer DSC-7 instrument (calibrated with indium) interfaced to a Perkin-Elmer TAC 7/DX Thermal Analysis Controller. Polarized optical microscopy analyses were performed using either a Nikon Eclipse E600 POL or Nikon Labophot-2 POL polarized microscope fitted with Linkam LTS 350 hot stages. Electroclinic tilt measurements were performed on samples aligned in rubbed polyimide/ITO coated glass cells with a spacing of 4 $\pm$ 0.5 μm (E.H.C., Japan). The film thickness was determined for each sample based on the capacitance of the empty cell using a Displaytech APT-III polarization testbed. Electroclinic tilt angles θ were determined by polarized microscopy as a function of E using a 0.1 Hz square wave ac field. Tilt angle values were taken as half the rotation between the two optical extinction positions corresponding to opposite signs of E. The electroclinic coefficient e_c at a given reduced temperature $T - T_C$ was determined according to eqn (1) from the linear region of a plot of θ *vs.* E; good least-squares fits ($R^2 \geqslant 0.98$) were obtained in all cases. Spontaneous polarizations were measured on the same aligned samples by the triangular wave method using a Displaytech APT-III polarization testbed in conjunction with the Linkam hot stage.[50] X-Ray scattering experiments were performed with Ni-filtered CuK_α radiation (wavelength 1.5418 Å). Small angle scattering data from unaligned samples (filled into Mark capillary tubes of 0.7 mm diameter) were obtained using a Kratky compact camera (A. Paar) equipped with a temperature controller (A. Paar) and a one-dimensional electronic detector (M. Braun).

Acknowledgements

We thank the Natural Sciences and Engineering Research Council of Canada (Discovery Grant to R.P.L., Postgraduate Scholarships to C.S.H., and Postdoctoral Fellowship to J.C.R.), the Canada Foundation for Innovation and the Deutsche Forschungsgemeinschaft (DFG) for support of this work.

References

1 C. Bahr, in *Chirality in Liquid Crystals*, ed. H.-S. Kitzerow and C. Bahr, Springer Verlag, New York, 2001; N. A. Clark and S. T. Lagerwall, in *Ferroelectric Liquid Crystals: Principles, Properties and Applications*, ed. J. W. Goodby, R. Blinc, N. A. Clark, S. T. Lagerwall, M. A. Osipov, S. A. Pikin, T. Sakurai, K. Yoshino and B. Zeks, Gordon and Breach, Philadelphia, 1991, p. 84.
2 S. Garoff and R. B. Meyer, *Phys. Rev. Lett.*, 1977, **38**, 848.
3 I. Abdulhalim and G. Moddel, *Liq. Cryst.*, 1991, **9**, 493.
4 G. Andersson, I. Dahl, L. Komitov, S. T. Lagerwall, K. Skarp and B. Stebler, *J. Appl. Phys.*, 1989, **66**, 4983.
5 G. Andersson, I. Dahl, W. Kuczynski, S. T. Lagerwall, K. Skarp and B. Stebler, *Ferroelectrics*, 1988, **84**, 285.
6 P. A. Williams, N. A. Clark, M. B. Ros, D. M. Walba and M. D. Wand, *Ferroelectrics*, 1991, **121**, 143.
7 B. R. Ratna, G. P. Crawford, S. Krishna Prasad, J. Naciri, P. Keller and R. Shashidhar, *Ferroelectrics*, 1993, **148**, 425.
8 M. Redmond, H. Coles, E. Wischerhoff and R. Zentel, *Ferroelectrics*, 1993, **148**, 323.
9 J. Naciri, J. Ruth, G. Crawford, R. Shashidhar and B. R. Ratna, *Chem. Mater.*, 1995, **7**, 1397.
10 G. P. Crawford, J. Naciri, R. Shashidhar and B. R. Ratna, *Jpn. J. Appl. Phys.*, 1996, **35**, 2176.
11 F. Giesselmann, P. Zugenmaier, I. Dierking, S. T. Lagerwall, B. Stebler, M. Kaspar, V. Hamplova and M. Glogarova, *Phys. Rev. E*, 1999, **60**, 598.
12 M. S. Spector, P. A. Heiney, J. Naciri, B. T. Weslowski, D. B. Holt and R. Shashidhar, *Phys. Rev. E*, 2000, **61**, 1579.
13 N. A. Clark, T. Bellini, R.-F. Shao, D. Coleman, S. Bardon, D. R. Link, J. E. Maclennan, X.-H. Chen, M. D. Wand, D. M. Walba, P. Rudquist and S. T. Lagerwall, *Appl. Phys. Lett.*, 2002, **80**, 4097.
14 J. P. F. Lagerwall, F. Giesselmann and M. D. Radcliffe, *Phys. Rev. E*, 2002, **66**, 031703.
15 O. E. Panarina, Y. P. Panarin, J. K. Vij, M. S. Spector and R. Shashidhar, *Phys. Rev. E*, 2003, **67**, 051709.
16 J. Naciri, C. Carboni and A. K. George, *Liq. Cryst.*, 2003, **30**, 219.
17 M. Krueger and F. Giesselmann, *Phys. Rev. E*, 2005, **71**, 041704.
18 N. Hayashi, T. Kato, A. Fukuda, J. K. Vij, Y. P. Panarin, J. Naciri, R. Shashidhar, S. Kawada and S. Kondoh, *Phys. Rev. E*, 2005, **71**, 041705.
19 J. P. F. Lagerwall and F. Giesselmann, *Chem. Phys. Chem.*, 2006, **7**, 20.
20 H. Stegemeyer, R. Meister, U. Hoffmann, A. Sprick and A. Becker, *J. Mater. Chem.*, 1995, **5**, 2183.
21 K. Saxena, L. Beresnev, L. Blinov, S. Pikin and W. Haase, *Ferroelectrics*, 1998, **213**, 73.
22 L. Beresnev, A. Biradar, W. Dultz, S. Pikin and W. Haase, *Mol. Cryst. Liq. Cryst.*, 1997, **299**, 525.
23 J. S. Kang, D. A. Dunmur, C. J. Booth, J. W. Goodby and K. J. Toyne, *Liq. Cryst.*, 1996, **20**, 109.
24 R. P. Lemieux, *Acc. Chem. Res.*, 2001, **34**, 845.
25 The polarization power is a measure of the propensity of a chiral dopant to induce a spontaneous polarization in an achiral SmC liquid crystal host: K. Siemensmeyer and H. Stegemeyer, *Chem. Phys. Lett.*, 1988, **148**, 409.
26 C. S. Hartley, C. Lazar, M. D. Wand and R. P. Lemieux, *J. Am. Chem. Soc.*, 2002, **124**, 13513.
27 T. Hegmann and R. P. Lemieux, *J. Mater. Chem.*, 2002, **12**, 3368.
28 G. P. Crawford, R. E. Geer, J. Naciri, R. Shashidhar and B. R. Ratna, *Appl. Phys. Lett.*, 1994, **65**, 2937.
29 A. G. Rappaport, P. A. Williams, B. N. Thomas, N. A. Clark, M. B. Ros and D. M. Walba, *Appl. Phys. Lett.*, 1995, **67**, 362.
30 J. V. Selinger, J. Xu, R. L. B. Selinger, B. R. Ratna and R. Shashidhar, *Phys. Rev. E*, 2000, **62**, 666.
31 The e_c value of 0.15 deg μm V^{-1} at $x_1 = 0.04$ measured in this study is *ca.* twice the value measured in our original study,[27] which is likely due to a weighing error. Given that e_c measurements were carried out over a range of x_1 values, and the quality of the least-squares fit shown in Fig. 1, we are confident of the value reported in this study.
32 D. Vizitiu, C. Lazar, B. J. Halden and R. P. Lemieux, *J. Am. Chem. Soc.*, 1999, **121**, 8229.
33 R. Bartolino, J. Doucet and G. Durand, *Ann. Phys.*, 1978, **3**, 389.
34 K. Ohno, M. Ushioda, S. Salto and K. Miyazawa, *Eur. Pat. Appl.*, EP 313991 A2, 1988.

35 C. Bahr, G. Heppke and U. Klemke, *Ber. Bunsen-Ges. Phys. Chem.*, 1991, **95**, 761.
36 G. P. Crawford, J. Naciri, R. Shashidhar, P. Keller and B. R. Ratna, *Mol. Cryst. Liq. Cryst.*, 1995, **263**, 223.
37 L. Beresnev, L. Blinov, S. Grossmann, K. Saxena and W. Haase, *Ferroelectrics*, 1997, **200**, 51.
38 C. C. Huang and S. C. Lien, *Phys. Rev. E*, 1985, **31**, 2621.
39 B. R. Ratna, R. Shashidhar, G. G. Nair, S. K. Prasad, C. Bahr and G. Heppke, *Phys. Rev. A*, 1988, **37**, 1824.
40 S. K. Prasad, V. N. Raja, D. S. Shankar Rao, G. G. Nair and M. E. Neubert, *Phys. Rev. A*, 1990, **42**, 2479.
41 B. Heinrich and D. Guillon, *Mol. Cryst. Liq. Cryst.*, 1995, **268**, 21.
42 C. Bahr and G. Heppke, *Phys. Rev. Lett.*, 1990, **65**, 3297.
43 T. Hegmann and R. P. Lemieux, unpublished results.
44 L. D. Landau, *Statistical Physics*, Pergamon Press, Oxford, 1980.
45 R. J. Birgeneau, C. W. Garland, A. R. Kortan, J. D. Litster, M. Meichle, B. M. Ocko, C. Rosenblatt, L. J. Yu and J. Goodby, *Phys. Rev. A*, 1983, **27**, 1251.
46 S. Diele, *Ber. Bunsen-Ges. Phys. Chem.*, 1993, **97**, 1326.
47 S. T. Lagerwall, *Ferroelectric and Antiferroelectric Liquid Crystals*, Wiley-VCH, Weinheim, 1999.
48 D. Hermann, L. Komitov, S. T. Lagerwall, B. Stebler, R. Shashidhar, J. V. Selinger and F. Giesselmann, *Ferroelectrics*, 1996, **181**, 371.
49 D. Vizitiu, C. Lazar, J. P. Radke, C. S. Hartley, M. A. Glaser and R. P. Lemieux, *Chem. Mater.*, 2001, **13**, 1692.
50 K. Miyasato, S. Abe, H. Takezoe, A. Fukuda and E. Kuze, *Jpn. J. Appl. Phys.*, 1983, **22**, L661.